Cellular/Molecular

Rapid Release of Ca^{2+} from Endoplasmic Reticulum Mediated by Na^{+}/Ca^{2+} Exchange

Che-Hsiung Liu,[1] Zijing Chen,[2] Megan K. Oliva,[3] Junjie Luo,[2] Simon Collier,[3] Craig Montell,[2] and Roger C. Hardie[1]

[1]Department of Physiology Development and Neuroscience, Cambridge University, Cambridge, CB2 3EG, United Kingdom, [2]Department of Molecular, Cellular, and Developmental Biology, University of California, Santa Barbara, Santa Barbara, California 93106-9625, and [3]Department of Genetics, Cambridge University, Cambridge, CB2 3EH, United Kingdom

Phototransduction in *Drosophila* is mediated by phospholipase C (PLC) and Ca^{2+}-permeable TRP channels, but the function of endoplasmic reticulum (ER) Ca^{2+} stores in this important model for Ca^{2+} signaling remains obscure. We therefore expressed a low affinity Ca^{2+} indicator (ER-GCaMP6-150) in the ER, and measured its fluorescence both in dissociated ommatidia and *in vivo* from intact flies of both sexes. Blue excitation light induced a rapid (tau ~0.8 s), PLC-dependent decrease in fluorescence, representing depletion of ER Ca^{2+} stores, followed by a slower decay, typically reaching ~50% of initial dark-adapted levels, with significant depletion occurring under natural levels of illumination. The ER stores refilled in the dark within 100–200 s. Both rapid and slow store depletion were largely unaffected in $InsP_3$ receptor mutants, but were much reduced in *trp* mutants. Strikingly, rapid (but not slow) depletion of ER stores was blocked by removing external Na^{+} and in mutants of the Na^{+}/Ca^{2+} exchanger, CalX, which we immuno-localized to ER membranes in addition to its established localization in the plasma membrane. Conversely, overexpression of *calx* greatly enhanced rapid depletion. These results indicate that rapid store depletion is mediated by Na^{+}/Ca^{2+} exchange across the ER membrane induced by Na^{+} influx via the light-sensitive channels. Although too slow to be involved in channel activation, this Na^{+}/Ca^{2+} exchange-dependent release explains the decades-old observation of a light-induced rise in cytosolic Ca^{2+} in photoreceptors exposed to Ca^{2+}-free solutions.

Key words: **calcium; NCX; photoreceptor; TRP**

Significance Statement

Phototransduction in *Drosophila* is mediated by phospholipase C, which activates TRP cation channels by an unknown mechanism. Despite much speculation, it is unknown whether endoplasmic reticulum (ER) Ca^{2+} stores play any role. We therefore engineered flies expressing a genetically encoded Ca^{2+} indicator in the photoreceptor ER. Although NCX Na^{+}/Ca^{2+} exchangers are classically believed to operate only at the plasma membrane, we demonstrate a rapid light-induced depletion of ER Ca^{2+} stores mediated by Na^{+}/Ca^{2+} exchange across the ER membrane. This NCX-dependent release was too slow to be involved in channel activation, but explains the decades-old observation of a light-induced rise in cytosolic Ca^{2+} in photoreceptors bathed in Ca^{2+}-free solutions.

Introduction

Phototransduction in microvillar photoreceptors is mediated by a G-protein-coupled phospholipase C (PLC), which hydrolyzes phosphatidyl inositol (4,5) bisphosphate ($PIP_{2)}$ to generate diacylglycerol and inositol (1,4,5) trisphosphate ($InsP_3$; for reviews, see: Katz and Minke, 2009; Fain et al., 2010; Hardie, 2012; Montell, 2012; Hardie and Juusola, 2015; Katz and Minke, 2018; Voolstra and Huber, 2020). In *Drosophila* photoreceptors, activation of PLC leads to opening of two related Ca^{2+}-permeable nonselective cation channels: TRP (*transient receptor potential*) and TRP-like (TRPL) in the microvillar membrane (Niemeyer et al., 1996; Reuss et al., 1997). TRP is the founding member of the TRP ion channel superfamily (Montell and Rubin, 1989; Hardie and Minke, 1992; Minke, 2010; Hardie, 2011; Montell, 2011), so named because the light response in *trp* mutants is transient, decaying rapidly to baseline during maintained illumination (Cosens and Manning, 1969; Minke et al., 1975). Because the most familiar product of PLC activity is $InsP_3$, it was initially thought that activation of the TRP/TRPL channels required

Received Nov. 8, 2019; revised Feb. 4, 2020; accepted Feb. 12, 2020.

Author contributions: C.-H.L., Z.C., C.M., and R.C.H. designed research; C.-H.L., Z.C., M.K.O., J.L., S.C., and R.C.H. performed research; C.M. contributed unpublished reagents/analytic tools; Z.C., C.M., and R.C.H. analyzed data; C.-H.L., Z.C., C.M., and R.C.H. wrote the paper.

The authors declare no competing financial interests.

This work was supported by BBSRC BB/M007006/1 (R.C.H., C.-H.L.); EY010852 from the NIH (C.M.); Newton International Fellowship NF150362 from the Royal Society and Marie-Skłodowska-Curie Fellowship 701397 from the European Union' Horizon 2020 research and innovation program (M.K.O.).We thank Dr. Tim Ryan for providing ER-GCaMP6-150 cDNA, the Cambridge Fly Facility for maintenance of fly stocks, and the laboratory of Dr. Cahir O'Kane for support and helpful discussions.

Correspondence should be addressed to Roger C. Hardie at rch14@cam.ac.uk.

https://doi.org/10.1523/JNEUROSCI.2675-19.2020

release of Ca^{2+} from endoplasmic reticulum (ER) stores via $InsP_3$ receptors ($InsP_3Rs$) and that in the absence of Ca^{2+} influx via TRP channels the stores depleted leading to the response decay (Minke and Selinger, 1991; Hardie and Minke, 1993). However, it was subsequently found that phototransduction was intact in $InsP_3R$ mutants (Acharya et al., 1997; Raghu et al., 2000), whereas response decay in *trp* mutants was associated with severe depletion of PIP_2. This suggested an alternative explanation of the *trp* decay phenotype, namely failure of Ca^{2+}-dependent inhibition of PLC and the consequent runaway consumption of its substrate, PIP_2 (Hardie et al., 2001). Nevertheless, a role for $InsP_3$ and Ca^{2+} stores in *Drosophila* phototransduction remains debated. For example, a recent study reported that sensitivity to light was attenuated by RNAi knockdown of $InsP_3R$ (Kohn et al., 2015), although we were unable to confirm this using either RNAi or null $InsP_3R$ mutants (Bollepalli et al., 2017).

Relevant to this debate, Ca^{2+} imaging reveals a small, but significant light-induced rise in cytosolic Ca^{2+} in photoreceptors bathed in Ca^{2+}-free solutions (Peretz et al., 1994; Hardie, 1996; Cook and Minke, 1999; Kohn et al., 2015). Although some have attributed this to $InsP_3$-induced Ca^{2+} release from the ER (Cook and Minke, 1999; Kohn et al., 2015), we found that the rise was unaffected in $InsP_3R$ mutants but was dependent on Na^+/Ca^{2+} exchange (Hardie, 1996; Asteriti et al., 2017; Bollepalli et al., 2017). This suggested that the Ca^{2+} rise was due to Na^+/Ca^{2+}exchange following Na^+ influx associated with the light response. However, it is difficult to understand how such a Ca^{2+} rise could be achieved by Na^+/Ca^{2+} exchange across the plasma membrane when extracellular Ca^{2+} was buffered to low nanomolar levels. The source of the Ca^{2+} rise in Ca^{2+}-free bath thus remains unresolved, and to date there have been no measurements of ER store Ca^{2+} levels in *Drosophila* photoreceptors. To address this, we generated flies expressing a low-affinity GCaMP6 variant in the ER lumen (de Juan-Sanz et al., 2017). Using this probe we demonstrate and characterize a rapid light-induced depletion of ER Ca^{2+}, which, like the cytosolic Ca^{2+} signal in Ca^{2+}-free bath, was unaffected by $InsP_3R$ mutations, but dependent on Na^+ influx and the CalX Na^+/Ca^{2+} exchanger. Our results indicate that the exchanger is also expressed on the ER membrane, that the Na^+ influx associated with the light-induced current leads to Ca^{2+} extrusion from the ER by Na^+/Ca^{2+}exchange and that this accounts for the rise in cytosolic Ca^{2+} observed in Ca^{2+}-free solutions.

Materials and Methods

Fly stocks

Fruit flies (*Drosophila melanogaster*) were reared on standard medium (for recipe, see Randall et al., 2015). Unless otherwise stated, flies were reared at room temperature (21–23°C) in normal room light on a 12h dark/light cycle. For dissociated ommatidia, we used newly eclosed (<2 h) adults; for *in vivo* deep pseudopupil measurements flies were 1–7 d old unless otherwise stated. Both male and female flies were used with no apparent difference.

We used the following stocks: (1) trp^{343}-null mutant lacking TRP channels (Montell and Rubin, 1989; Scott et al., 1997; Wang et al., 2005a); (2) $norpA^{P24}$-null mutant of PLC (Pearn et al., 1996); (3) $calx^A$, severe loss of function mutant of the Na^+/Ca^{2+} exchanger with no detectable exchanger activity in the photoreceptors (Wang et al., 2005b); (4) $calx^B$, a strong mutant allele expressing negligible levels of the Na^+/Ca^{2+} exchanger (Wang et al., 2005b; Chen et al., 2015); (5) *ninaE-calx/CyO*, flies overexpressing a wild-type *calx* transgene under control of the *ninaE* (*Rh1*) promoter, abbreviated to *pCalX* (Wang et al., 2005b); and (6) $l(3)itpr^{90B.0}$, a larval lethal null mutant of the $InsP_3$ receptor: referred to as *itpr* (Venkatesh and Hasan, 1997). All these lines were on a white-eyed (w^{1118}) background; however, *itpr* has a strong mini-w^+ transgene inserted near the *itpr* locus conferring a red eye pigmentation at least as dark as in wild-type flies. Because this obscured *in vivo* fluorescence from the deep pseudopupil (DPP), the mini-w^+ transgene in *itpr* mutants was mutated using CRISPR-Cas9 methodology for flies used for *in vivo* measurements (see "Generation of *white eraser* flies").

Because *trp*, *norpA*, and *calx* mutants all undergo light-dependent retinal degeneration (Stark et al., 1989; Wang et al., 2005b; Sengupta et al., 2013), care was taken to use young flies (≤2 d old) in which the retina was intact as judged by the appearance of the DPP. For each of these mutants, measurements were also made on flies reared in darkness and because no difference in behavior was noted, the results were pooled.

Generation of ER-GCaMP6-150 and RGECO1 flies

ER-GCaMP6-150 (cDNA obtained from Dr. Tim Ryan) is a low affinity GCaMP6 variant, which is targeted to the ER lumen using the N-terminal signal peptide of calreticulin and the C-terminal KDEL retention motif (de Juan-Sanz et al., 2017). RGECO1 (cDNA from Addgene) is a red fluorescent genetically encoded Ca^{2+} indicator with a dissociation constant (K_D) of 450 nM and a 12-fold dynamic range (Dana et al., 2016), which we targeted to the microvilli by adding a C-terminal tag consisting of the C-terminal (amino acids 863–1045) of *norpA* PLC. The constructs were cloned into the pCaSpeR4 vector, which contains a mini-w^+ gene as transfection marker and the *ninaE* (*Rh1*) promoter that drives expression exclusively in photoreceptors R1-6. The final constructs (*ninaE-ER-GCaMP6-150*, abbreviated to *ER-150* and *ninaE-RGECO1-norpACT*, referred to as *RGECO1*) were injected into w^{1118} embryos and transformants recovered on second and third chromosomes. The transgenes were crossed into various genetic backgrounds, all on a w^{1118} background, as required. Flies used for experiments contained just one copy of *ER-150* or *RGECO1* and had a pale orange eye color from the mini-w^+ transfection marker, which was weak enough not to compromise fluorescence measurements from the DPP

To express *ER-150* in $InsP_3R$ null (*itpr*) whole-eye mosaics: *ER-150/Cy; FRT82B, l(3)itpr$^{90B.0}$/TM6* flies were crossed to *yw;P{w+, ey-Gal4,UAS-FLP}/CyO;P{ry+,FRT82B}P{w+,GMR-hid},3CLR/TM6* (Bloomington stock #5253). Non-*Cy* and non-*TM6* F1 from this cross have *itpr* homozygote null mosaic eyes (Stowers and Schwarz, 1999; Raghu et al., 2000; Bollepalli et al., 2017) and express ER-150 in R1-6 photoreceptors.

Generation of *white eraser* flies

To remove expression of the mini-w^+ transfection marker and create white-eyed flies in *itpr* mutants used for *in vivo* DPP measurements and in *ER-150* flies used for immunostaining, we designed a tool called *white eraser* (*WE*). The DNA construct used for creating the *WE* strain contains: (1) two homologous DNA fragments corresponding to the mini-w^+ for HDR (arm 1 corresponds to nucleotides –2895 in mini-w^+, and arm 2 corresponds to nucleotides 2944–4136 in mini-w^+); (2) *DsRed*, which is flanked by the homologous arms and inserts in mini-w^+ to create mini-w^{DsRed}; (3) two copies of two gRNAs targeting the mini-w^+ marker, expressed under control of the *U6* promoter [targets CCGCAGTCCGATCATCGGATAGG (gRNA1) and CTTCTTCAAC TGCCTGGCGCTGG (gRNA2) in the mini-w^+ gene]; (4) GFP expressed under control of the *3xP3* promoter to distinguish the *WE* transgene from the mutated mini-w^+; and (5) a transgene encoding Cas9, which is expressed under the control of the *actin5C* (*Act5C*) promoter. To eliminate mini-w^+ expression, we crossed flies with the mini-w^+ marker to the *WE* flies. The progeny can have either of two types of the mutations in mini-w^+: mini-w^{DsRed} and mini-w^* The mini-w^{DsRed} is because of homology directed repair (HDR) using the template in the *WE* transgene (Fig. 1). The mini-w^* is generated by non-homologous end joining (NHEJ), which creates an indel in the mini-w^+ (Fig. 1). Approximately 73% of the mini-w^+ were mutated in our tests. The probability of mutating the mini-w^+ was not dependent on the location of the target transgene. However, the probability of converting mini-w^+ into mini-w^{DsRed} is dependent on the distance between the *WE* insertion site and the target transgene. If the distance is <4 Mbp, ~16% of mini-*w* are converted to mini-w^{DsRed} and 57% of mini-w^+

are converted to *mini-w*. If the distance is >4 Mbp, then nearly all of the mutants are* mini-w*.

Fluorescence measurements

Fluorescence measurements were made as previously described (Satoh et al., 2010; Asteriti et al., 2017) on an inverted Nikon TE300 microscope (Nikon) from dissociated ommatidia or *in vivo* by imaging the DPP in intact flies immobilized with low melting point wax in plastic pipette tips. For ER-150 excitation light (470 nm) was delivered from a blue power LED (Cairn Research) and fluorescence observed using 515 nm dichroic and OG515 long-pass filters. RGECO1 fluorescence was excited and imaged via a white-power LED and an RFP filter set. Fluorescent images were sampled and analyzed using an Orca-Flash4.0 camera and HCImagelive software (Hamamatsu); but for most experiments fluorescence of whole ommatidia (via 40× oil objective), or DPP (20× air objective) was directly measured via a photomultiplier tube (Cairn Research), sampled at up to 1 kHz and analyzed with pCLAMP v10 software (Molecular Devices). Following each measurement, the ommatidium/fly was exposed to intense, photoequilibrating red (2–4 s, 640 nm ultra-bright LED) illumination to reconvert metarhodopsin (M) to rhodopsin (R), and allowed to dark adapt before the next measurement.

For two-pulse experiments, green light was supplied by a "warm-white" power LED (Cairn Research) filtered by a GG 475 filter (resulting λ_{max} 546 nm). The green illumination was calibrated in terms of effectively absorbed photons by measuring the rate at which it converted M to R spectrophotometrically, as previously described (Hardie et al., 2015).

Dissociated ommatidia were prepared from newly eclosed flies as previously described (Reuss et al., 1997; Katz et al., 2017) and plated in a chamber containing control bath with (in mM): 120 NaCl, 5 KCl, 10 *N*-tris-(hydroxymethyl)-methyl-2-amino-ethanesulfonic acid (TES), 4 $MgCl_2$, 1.5 $CaCl_2$, 25 proline, and 5 alanine, pH 7.15 (all chemicals from Sigma-Aldrich). For Ca^{2+}-free measurements, dissociated ommatidia were individually perfused with a Ca^{2+}-free solution (0 Ca^{2+}, 1 mM Na_2EGTA, otherwise as above) by a nearby (~20–50 μm) puffer pipette and measurements made ~20–45 s after perfusion onset. For Na^+-free solutions NaCl was substituted for equimolar *N*-methyl D-glucamine Cl (NMDG).

Immunocytochemistry

All immunostaining was performed using whole mounts of newly eclosed or 1-d-old adult eyes. To test whether a subset of CalX is present in the ER, we used ER-150 as an ER marker. Because pigment from the mini-w^+ transfection marker included in the *ER-150* transgene contributes to autofluorescence, we mutated the mini-w^+ transgene with the *WE*. We performed double staining using anti-CalX and anti-GFP, which recognized ER-150. For CalX staining in w^{1118} and $calx^B$, we used rabbit anti-CalX (Wang et al., 2005b), and TO-PRO-3 (ThermoFisher, T3605) at a 1:500 dilution was added as a nuclear counterstain during secondary antibody incubation. To conduct the immunostaining, we fixed whole flies in PBS (9 g/L NaCl, 144 mg/L KH_2PO_4 and 795 mg/L Na_2HPO_4, pH 7.4) plus 4% paraformaldehyde on ice for 2 h. After fixation, we dissected out the eyes in PBS + 0.1% Triton X-100, and incubated the samples in blocking buffer (100 mM Tris·HCl pH 7.5, 150 mM NaCl, 0.1% Triton X-100, 10% normal goat serum) at room temperature for 1 h. We subsequently incubated the samples with primary antibodies diluted in blocking buffer at 4°C for 2 d. After washing the samples three times in PBS + 0.1% Triton X-100, we incubated the samples with secondary antibodies at 4°C overnight. We washed the samples three times in PBS + 0.1% Triton X-100, and mounted them in VECTASHIELD (Vector Laboratories). We acquired images using a Zeiss LSM 700 confocal microscope with optical sections at 1 μm using a Plan-Apochromat 63× objective.

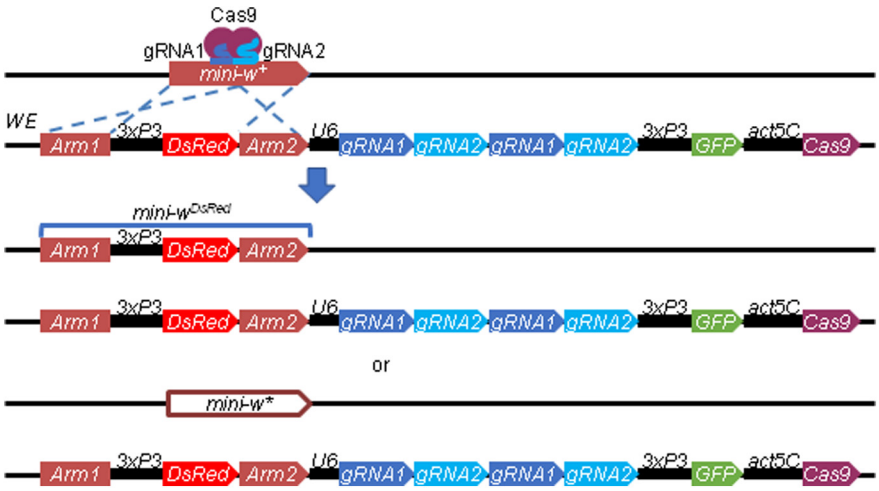

Figure 1. Creation of *WE* to mutate *mini-w*$^+$ transgenes. Genetic introduction of the WE insertion with a *mini-w*$^+$ transgene leads to mutation of the *mini-w*$^+$ either through HDR or NHEJ. The *WE* encodes two copies of two guide RNAs (*gRNA1* and *gRNA2*) expressed under control of the U6 promoter, and Cas9 expressed under control of the *actin5C* promoter. This can lead to HDR due to the two homology arms corresponding to the *mini-w*$^+$ transgene (blue dashed lines). If HDR takes place, DsRed, which is expressed under control of the 3xP3 promoter, is inserted in the *mini-w*$^+$, thereby creating the *mini-w*^{DsRed}. Alternatively, if NHEJ takes place, a mutation is introduced in the *mini-w*$^+$, creating *mini-w**. The 3xP3-GFP is a negative marker to distinguish the mutated transgene from *WE*.

Antibodies for immunostaining

Primary antibodies: 1:500 chicken anti-GFP (ThermoFisher, A10262) to recognize ER-150, 1:200 rabbit anti-Calnexin (Rosenbaum et al., 2006), 1:250 rabbit anti-CalX (Wang et al., 2005b) and 1:500 mouse anti-ATP5A (Abcam, ab14748). Secondary antibodies: 1:200 goat anti-chicken AlexaFluor 488 (ThermoFisher, A10262), 1:200 goat anti-rabbit AlexaFluor 568 (ThermoFisher, A11036), anti-mouse AlexaFluor 568 (ThermoFisher, A11004), and 1;200 goat anti-rabbit AlexaFluor 488 (ThermoFisher, A11008).

Experimental design and statistical analysis

Statistical tests (unpaired two-tailed *t* tests or one-way ANOVA with Tukey's *post hoc* test) were performed using GraphPad Prism (v5.0). Relevant *p* values and sample sizes are indicated on figures or in text. Figures show mean ± SEM for each group and also the individual values for each experiment. For measurements from dissociated ommatidia, we noted that most variability was between flies rather than between ommatidia from the same fly. Therefore data were collected from (typically) 3–5 ommatidia per fly and then averaged. Unless otherwise stated each data point on figure panels from dissociated ommatidia (see Fig. 3*C*,*D*) represents the average of ommatidia from one fly, and further statistics (*t* tests, etc.) were performed across these averages.

Results

Monitoring ER Ca^{2+} with ER-targeted GCaMP6-150

In order to monitor Ca^{2+} levels in ER stores, we targeted a low affinity GCaMP6 variant (K_D 150 μM Ca^{2+}) to the ER using a construct with the N-terminal signal peptide of calreticulin and a C-terminal KDEL retention motif (de Juan-Sanz et al., 2017). We engineered flies expressing this construct ("*ER-150*") in the major class of R1-6 photoreceptors using the *ninaE* (Rh1 rhodopsin) promoter. In fluorescent images of whole mounts or dissociated ommatidia, extensive "patchy" GCaMP fluorescence

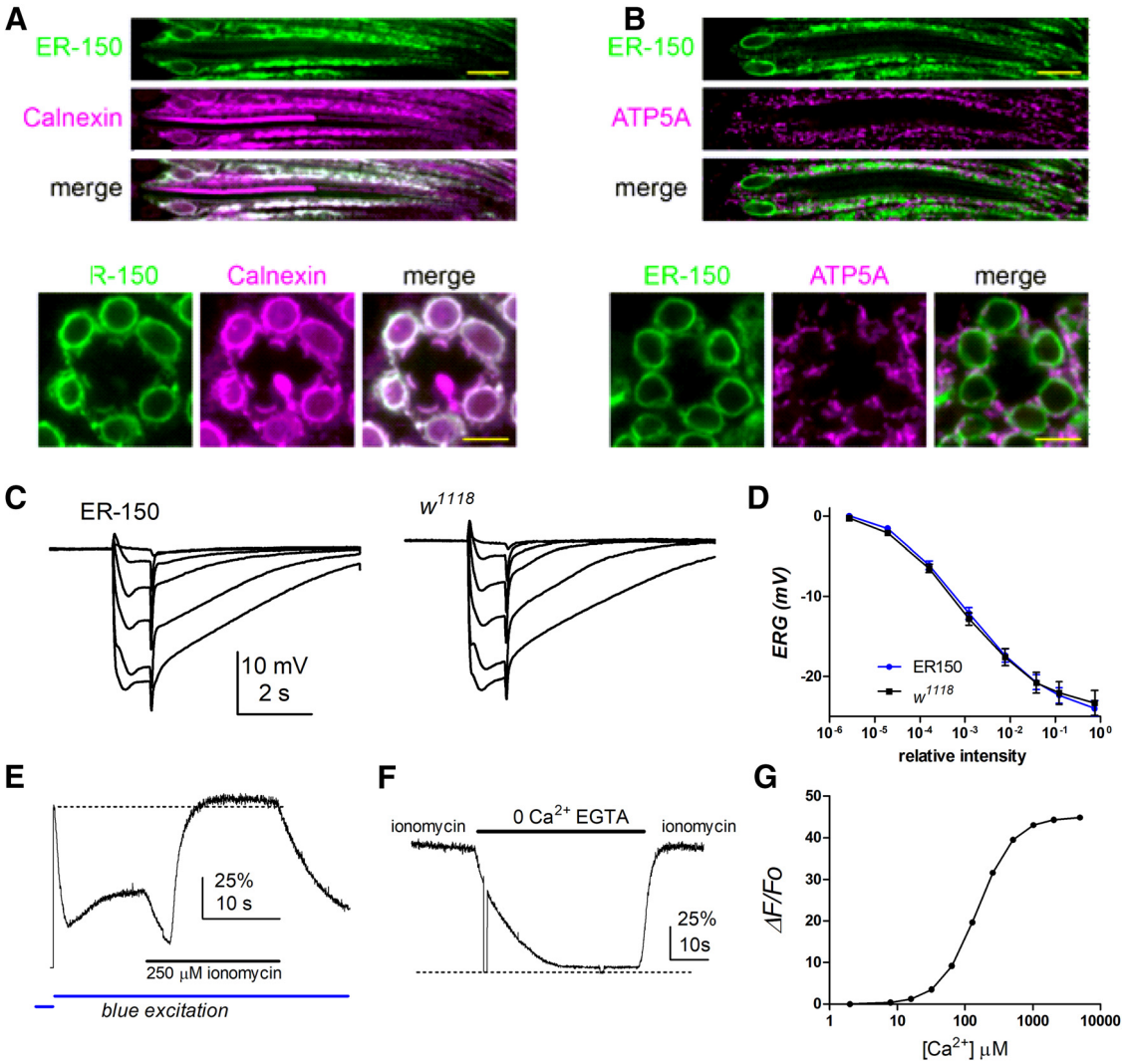

Figure 2. Expression and calibration of ER-150. ***A***, Optical sections of ommatidia from newly-eclosed flies expressing ER-150 colabeled with anti-GFP (to recognize ER-150; green) and anti-Calnexin (independent ER marker; magenta) show extensive co-localization (note that ER-150, under control of the *ninaE* promoter, is expressed only in R1-6 photoreceptor cells, but Calnexin is also expressed in R7 and R8 cells). Top, Longitudinal view. Scale bar, 10 μm. Below, Transverse view. Scale bar, 5 μm. ***B***, Similar optical sections colabeled with anti-GFP (ER-150; green) and a mitochondrial marker anti-ATP5a (magenta) indicate little or no co-localization. ***C***, Electroretinogram (ERG) responses to 1 s flashes of increasing intensity in ER-150 files and wild-type control (w^{1118}). ***D***, response intensity (V/log I) functions from maintained negative component of the ERG (average of final 100 ms of responses before the off transient; mean ± SEM, $n = 6$ flies). ***E***, Fluorescence measured from a dissociated wild-type ommatidium expressing ER-150. Following the rapid decay (store depletion) and partial recovery induced by the onset of the blue excitation light (Fig. 3*B*), the ommatidium was perfused with bath solution containing 250 μM ionomycin, 10 mM $CaCl_2$ (25 mM TES, pH 7.25). Fluorescence first decayed briefly before rapidly increasing slightly beyond the initial dark adapted F_0 (dotted line). ***F***, In an ommatidium already exposed to 250 μM ionomycin, subsequent perfusion with 0 Ca^{2+} (1 mM EGTA) solution rapidly reduced fluorescence to near zero (zero level, dotted line, indicated by brief breaks in the blue excitation), recovering rapidly on reperfusion with Ca^{2+}/ionomycin containing solution. ***G***, Theoretical calibration curve for ER-150 assuming a dynamic range of 45 Kd 150 μM and Hill coefficient of 1.6 (de Juan-Sanz et al., 2017).

could be seen throughout the R1-6 photoreceptor cell bodies, with particularly prevalent signal in perinuclear ER (Figs. 2, 3, 5). To confirm that ER-150 was targeted to the ER, we performed double labeling using anti-GFP to recognize ER-150, and an antibody against Calnexin, which localizes to the ER (Schrag et al., 2001; Rosenbaum et al., 2006). As expected, we found that ER-150 and Calnexin colocalized extensively in R1-6 photoreceptors (Fig. 2*A*). We also performed double labeling using the mitochondrial marker ATP5A and found little or no indication of colocalization with ER-150 (Fig. 2*B*). Expression of the *ER-150* transgene had no discernible effect on photoreceptor structure at the light microscopic level (Figs. 2, 5) or physiology as assessed by electroretinogram (Fig. 2*C*,*D*).

To calibrate the maximum and minimum fluorescence from the ER-150 probe, dissociated ommatidia were perfused with bath solution supplemented with the Ca^{2+} ionophore ionomycin (250 μM, pH 7.25) and 10 mM Ca^{2+} (Fig. 2*E*). This resulted in only a small (~10–20%) increase in fluorescence above the initial resting value, and even some of this might be attributed to an expected pH increase (de Juan-Sanz et al., 2017). This implies that resting Ca^{2+} concentration in the stores was close to saturating levels for ER-150, indicating a resting store Ca^{2+} concentration of at least ~0.5 mM (Fig. 2*G*). When ionomycin-treated ommatidia were subsequently exposed to Ca^{2+}-free (1 mM EGTA) bath, fluorescence rapidly decayed to very low levels, recovering rapidly on reperfusion with ionomycin/Ca^{2+} containing solution (Fig. 2*F*). After background correction, the dynamic range (F_{max}/F_{min}) of the probe measured in this way was 46.2 ± 7.8-fold (mean, SEM, $n = 4$), in excellent agreement with the published *in vitro* value of 45 (de Juan-Sanz et al., 2017).

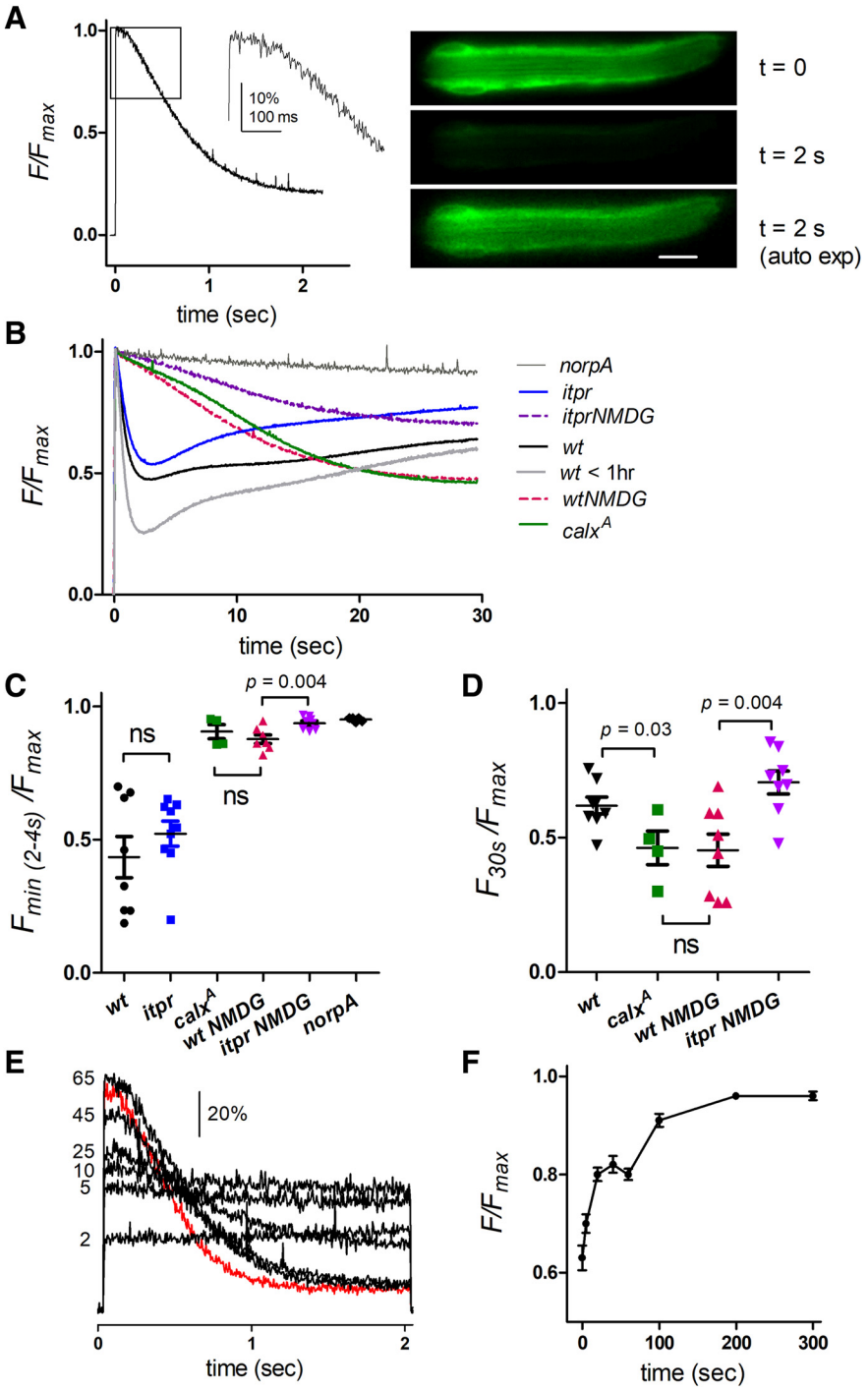

Figure 3. Measuring ER luminal Ca^{2+} levels in dissociated ommatidia. ***A***, Normalized fluorescence from wild-type ommatidium expressing ER-150: after a brief ~100 ms delay, store Ca^{2+} rapidly declined in response to the saturating blue excitation. Right, Images from Movie 1 (20 Hz) at onset of blue ($t = 0$) and after 2 s; 2 s image also shown after adjusting auto-exposure to facilitate comparison with $t = 0$ image. Scale bar 10 μM. ***B***, ER-150 fluorescence from dissociated ommatidia on a longer time scale (averaged traces from 14 to 30 ommatidia from 3 to 8 flies per trace). Wild-type shows rapid depletion followed by partial refilling with two distinct phases during the maintained blue excitation; in very young flies (<1 h post-eclosion) depletion was more extensive. Rapid depletion, indistinguishable from wild-type was seen in ommatidia from null $InsP_3R$ mosaic eyes (*itpr*). Rapid depletion was blocked in the same ommatidia perfused with Na^+-free solution (130 $NMDG^+$ substituted for Na^+), leaving a much slower, but ultimately more profound depletion. Similar behavior was seen in mutants of the Na^+/Ca^{2+} exchanger ($calx^A$) in normal bath. This slow phase of store depletion was less pronounced in *itpr* mutants. In $norpA^{P24}$ there was no depletion beyond a slight decay due to bleaching. ***C***, ***D***, Statistics: mean ± SEM from traces as in ***B***, each point derived from the average trace (3–8 ommatidia) from one fly. ***C***, minimum values (normalized to F_{max}) reached during rapid depletion phase (2–4 s); *itpr* mutants were not significantly different (ns) from wild-type ($p = 0.33$, two-tailed *t* test), but rapid depletion was largely blocked after NMDG substitution and in $calx^A$ flies. ***D***, Slow depletion (values reached after 30 s) was slightly more pronounced in $calx^A$ mutants than wild-type, whereas after NMDG substitution, *itpr* mutants showed less slow depletion than wild-type (two-tailed *t* tests). ***E***, Refilling of store Ca^{2+} following depletion: repeated ER-150 fluorescence traces from one ommatidium after different times in the dark (2–65 s) following initial depletion (first, dark-adapted trace; red) and re-isomerization of M to R by red illumination. ***F***, Averaged time course of store refilling from such measurements (mean ± SEM, $n = 8$ ommatidia) showing recovery in two phases.

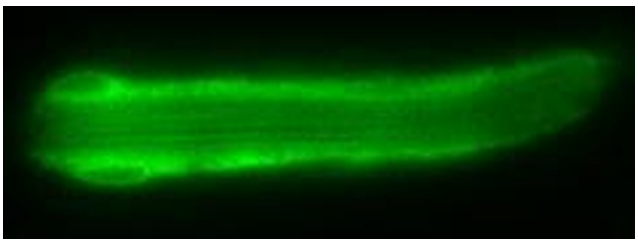

Movie 1. Twenty frames per second movie of initially dark-adapted, otherwise wild-type dissociated ommatidium expressing ER-150. The blue excitation light serves also as stimulus and induces rapid depletion of the ER Ca stores. Total duration of movie is 2 s. [View online]

ER-150 Ca^{2+} signals from dissociated ommatidia

In response to the blue excitation (a super-saturating stimulus for the photoreceptors), after a short delay of ~100 ms the initial ER-150 fluorescence in wild-type ommatidia decayed rapidly over ~2 s to, on average, ~50% of the initial level with an approximately exponential time course of <1 s (0.77 ± 0.13 s, mean ± SEM, $n = 30$ ommatidia from 8 flies). This decay was blocked in null mutants of PLC (*norpA*^{P24}) indicating that the ER Ca^{2+} stores were depleted as a consequence of activation of the phototransduction cascade (Fig. 3*A*,*B*). High frame rate movies (10–50 Hz) showed uniform decay of the fluorescence throughout the ommatidium (Fig. 3*A*; Movie 1), and for convenience measurements were subsequently made with photomultiplier tube measurements collecting fluorescence imaged from single ommatidia.

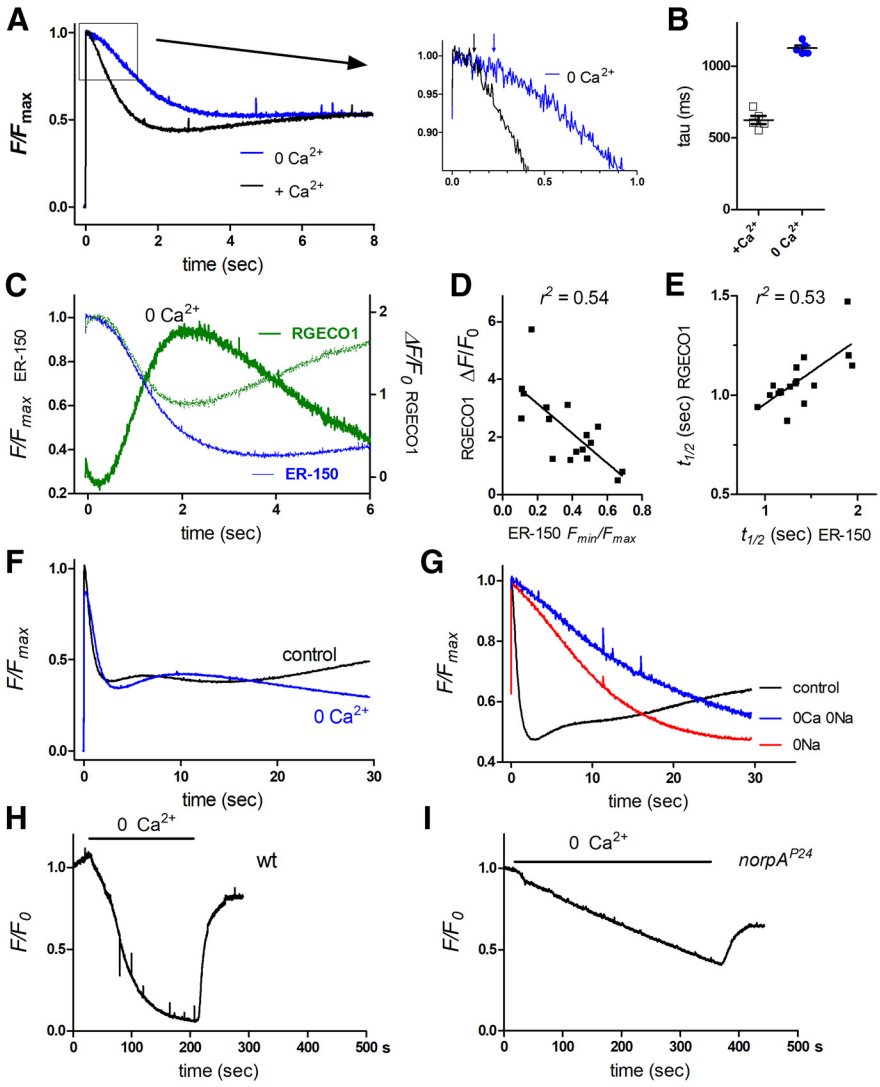

Figure 4. ER store depletion in dissociated ommatidia in Ca^{2+}-free solutions. ***A***, Normalized ER-150 fluorescence in response to blue excitation control bath and in the same ommatidia perfused for ~30 s with Ca^{2+}-free bath (0 Ca^{2+}, 1 mM EGTA). Average traces from five ommatidia in three otherwise wild-type flies. Inset (right), Expanded scale to show increase in latency (arrows). ***B***, Time constants (tau) of rapid depletion from exponential fits to decay. ***C***, Store depletion (ER-150 fluorescence, blue trace, expressed as F/F_{max}) and cytosolic Ca^{2+} (RGECO1 fluorescence; green trace expressed as $\Delta F/F_0$) measured from the same ommatidia (average of 17 ommatidia from 5 otherwise wild-type flies). Stippled green trace: RGECO1 data replotted after inverting and rescaling to compare time courses. ***D***, Peak RGECO1 $\Delta F/F_0$ values (cytosolic Ca^{2+}) from these ommatidia correlated strongly with the extent of store depletion (ER-150 F_{min}/F_{max} values) in the same ommatidium. ***E***, Time to 50% depletion ($t_{1/2}$ ER-150) in these ommatidia also correlated with the $t_{1/2}$ for the rise in cytosolic Ca^{2+}. ***F***, Store depletion (ER-150 fluorescence): averaged from 10 ommatidia from 2 wild-type flies in control bath and during 0 Ca^{2+} perfusion, monitored over 30 s. ***G***, Store depletion (ER-150 fluorescence) measured from wild-type ommatidia over 30 s in control bath, and same ommatidia during perfusion with 0 Na (130NMDG, 1.5 Ca, 4 Mg; $n = 8$) and 0Ca/0Na (130NMDG, 0Ca 1 mM EGTA, 4 Mg; $n = 3$). ***H***, ER-150 fluorescence (normalized to fluorescence at time 0) measured continuously during perfusion with 0 Ca^{2+} (1 mM EGTA) in a wild-type background; the ER stores depleted almost completely within ~3 min and then rapidly refilled on re-exposure to normal Ca^{2+} containing bath. ***I***, During 0 Ca^{2+} perfusion in a PLC-null (*norpA*^{P24}) background, store Ca^{2+} declined more slowly, recovering partially on reperfusion with Ca^{2+} containing bath.

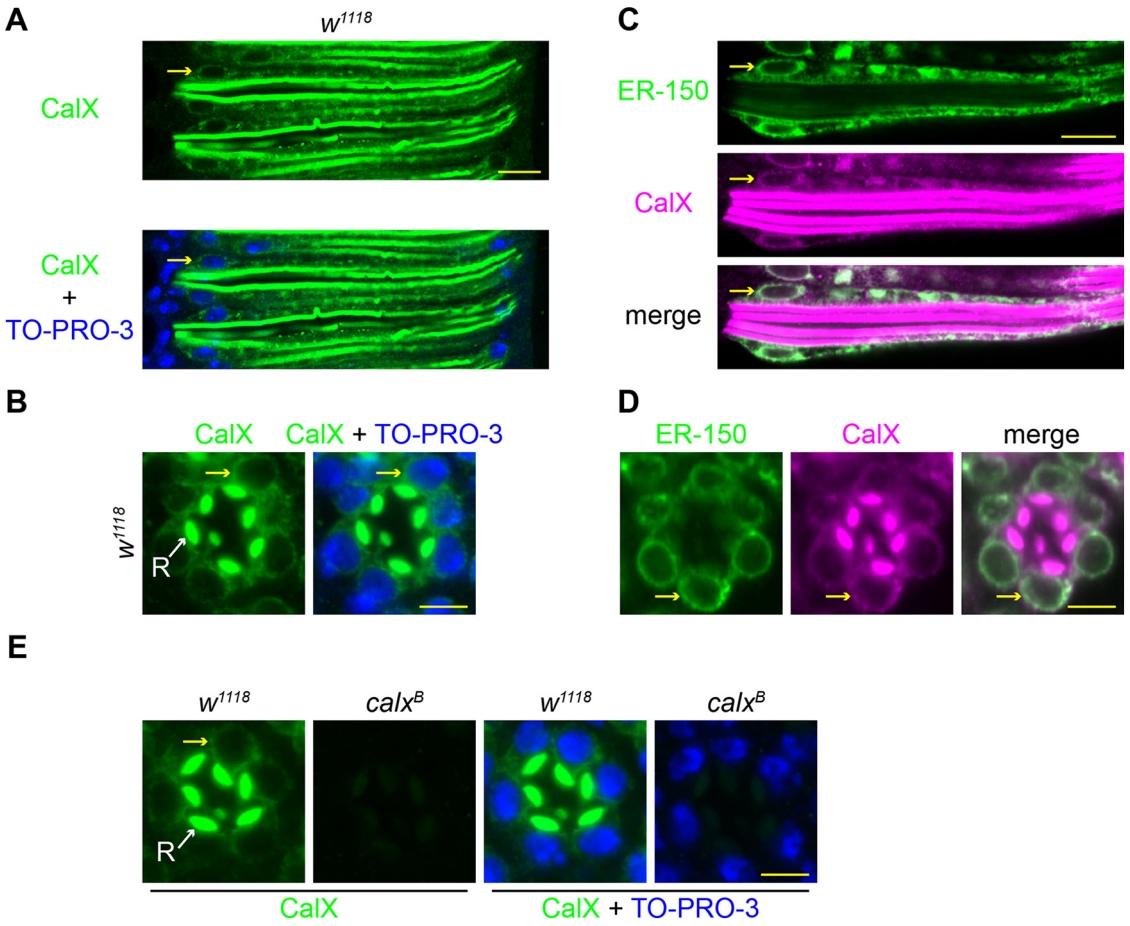

Figure 5. ER localization of CalX. ***A***, ***B***, Optical sections of ommatidia from newly eclosed w^{1118} flies costained with anti-CalX (green) and TO-PRO-3 (blue), which counterstains nuclei. Anti-CalX staining is observed in the rhabdomeres of R1-6 and to lesser extent R7 (small central rhabdomere). In addition, weaker, but clear staining was observed in the cell bodies including the perinuclear ER membrane (yellow arrows). ***A***, Longitudinal view. ***B***, Transverse view. ***C***, ***D***, Optical sections of single ommatidium from newly eclosed flies expressing ER-150 were costained with anti-GFP (ER-150 as ER marker; green) and anti-CalX (magenta). ***C***, Longitudinal view. ***D***, Transverse view. Merged images show extensive co-localization in the cell body. Yellow arrows indicate perinuclear (ER) staining. ***E***, Anti-CalX (green) and TO-PRO-3 staining controls for antibody specificity in 1-d-old flies. Anti-CalX staining is absent in both rhabdomere and cell body in the severe hypomorphic mutant $calx^B$. Scale bars: ***A***, ***C***, 10 μm; ***B***, ***D***, ***E***, 5 μm.

There was some variability in the extent (~20–80%) and speed of store depletion (tau 350–1200 ms) from fly to fly, with the most extensive rapid depletion occurring in ommatidia from very young flies (<1 h post eclosion) reared in room light (Fig. 3*B*). When fluorescence was tracked over longer time periods (30 s) there was usually a partial recovery indicating refilling of the stores during maintained blue excitation. Particularly in those ommatidia in which the stores had undergone more extensive rapid depletion, this could often be seen to occur in two phases (~5–10 and ~15–30 s; Fig. 3*B*). After photo-reisomerization of M to R with bright long wavelength light (see Materials and Methods) and return to the dark the fluorescence recovered fully over 2–3 min, again with two distinct phases (Figs. 3*E*,*F*).

Given that phototransduction in *Drosophila* is mediated by PLC, the most obvious explanation for the rapid light-induced store depletion might seem to be release of Ca^{2+} from the ER via $InsP_3$ receptors. However, when ER-150 was expressed in null mosaic eye mutants (*itpr*) of the only $InsP_3$ receptor gene in the *Drosophila* genome (Raghu et al., 2000), rapid store depletion persisted with similar time course and extent (Fig. 3*B*,*C*). This is perhaps not surprising, because the rise in cytosolic Ca^{2+} in *Drosophila* photoreceptors exposed to Ca^{2+}-free bath was also found to be unaffected in *itpr* mutants (Bollepalli et al., 2017), despite an earlier claim to the contrary (Kohn et al., 2015). However, just like the cytosolic Ca^{2+} rise seen in Ca^{2+}-free bath (Asteriti et al., 2017), the rapid light-induced store depletion was dependent on external Na^+ being severely attenuated in a reversible manner when perfused with solutions in which Na^+ was substituted for $NMDG^+$. This dependence on external Na^+ suggested that the rapid store depletion might be dependent on Na^+/Ca^{2+} exchange. In support of this, ER-150 fluorescence measured in $calx^A$, a severe *loss of function* mutant of the NCX Na^+/Ca^{2+} exchanger (Wang et al., 2005b), showed a very similar behavior to wild-type ommatidia perfused with Na^+-free solutions, with the loss of the rapid store depletion signal (Fig. 3*B*,*C*).

Nevertheless, despite the loss of rapid store depletion, under both these conditions (Na^+ substitution or $calx^A$ mutant), there was a much slower decay, which often eventually resulted in levels lower than in normal bath (mean ~45% of initial F_{max}). A similar slow phase was also observed in ommatidia from *itpr*-null mosaic eyes during perfusion with $NMDG^+$, although it appeared significantly less pronounced than in controls (Fig. 3*B*, *D*). Although the slow phase was only normally observed in dissociated ommatidia under conditions where Na^+/Ca^{2+}exchange was blocked, as described below (see "Monitoring ER Ca^{2+} stores *in vivo*") a similar delayed slow phase was routinely observed *in vivo* in intact flies.

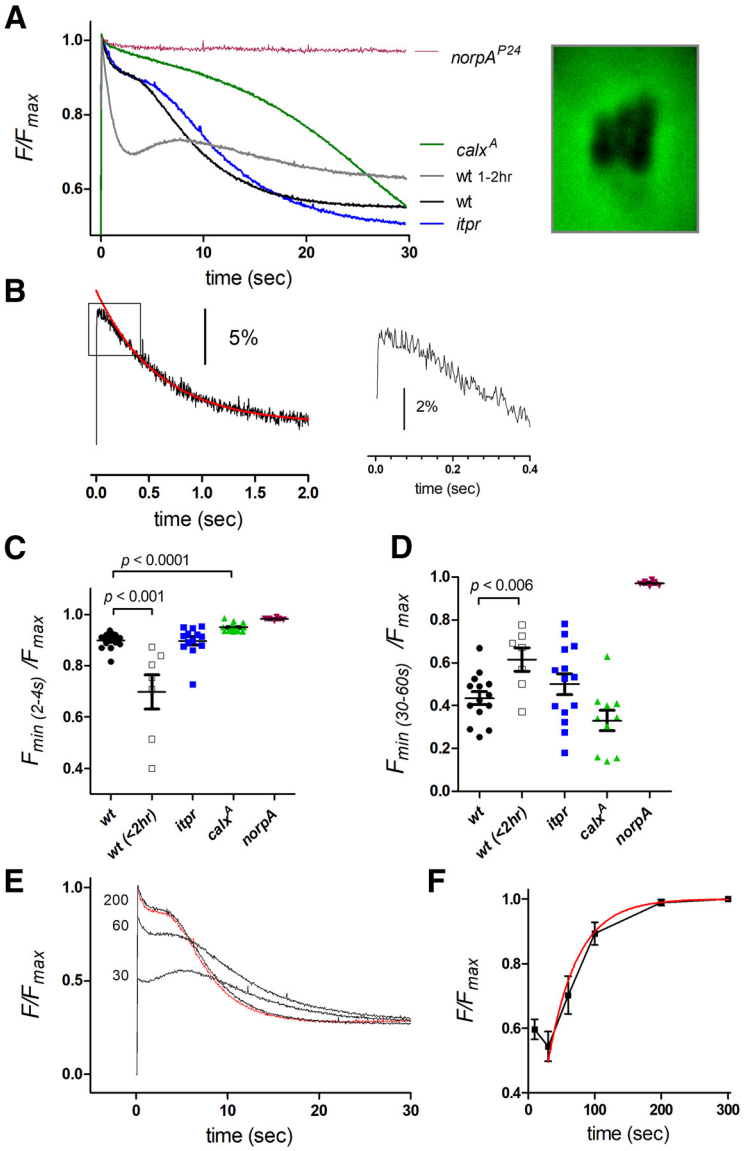

Figure 6. Monitoring ER store [Ca^{2+}] *in vivo* from ER-150 fluorescence in the deep pseudopupil. ***A***, ER-150 fluorescence traces from DPP (image right) in intact 1- to 5-d-old adult flies in wild-type (mean of traces from $n = 17$ flies), $calx^A$ ($n = 11$), *itpr* mosaic eyes ($n = 12$), $norpA^{P24}$ ($n = 6$), and also very young (<2 h) wild-type flies ($n = 6$). An initial rapid ~10% depletion, was suppressed in $calx^A$, but not in *itpr* mutants. A second slow phase of depletion was still present (albeit delayed) in $calx^A$, whereas in $norpA^{P24}$ there was no store depletion. ***B***, Rapid depletion from DPP of a single wild-type fly on faster time scale: fluorescence sampled at 500 Hz and averaged from 34 repeated episodes of blue excitation (with 4 s bright red illumination to re-isomerize M to R and 60 s dark adaptation between each episode). Inset (right), on a faster time base. The kinetics, including a ~100 ms delay, were similar to those recorded from dissociated ommatidia (compare Figs. 3, 4). Red curve, Exponential fit to the decay (τ = 590 ms). ***C***, ***D***, Statistics (mean ± SEM; each data point from a different fly) from traces as in ***A***. ***C***, Minimum value reached during rapid depletion phases (2-4 s); $calx^A$ mutants showed less depletion but *itpr* mutants were not significantly different from wild-type (one-way ANOVA with Tukey's post-test). ***D***, Minimum value reached after 30–60 s; neither *itpr* nor $calx^A$ mutants differed significantly from wild-type (one-way ANOVA, Tukey's post-test), but young (<2 h) wild-type flies now showed less long-term depletion (two-tailed *t* test with respect to older wild-type). ***E***, ER-150 fluorescence traces from a wild-type fly: red trace initial dark-adapted trace, subsequent traces measured after 30, 60, and 200 s dark recovery. ***F***, normalized store refilling time course (mean ± SEM, $n = 10$ flies, red curve, 1 exp fit, tau = 43.7 s) from such traces.

Ca^{2+} release from ER stores under Ca_o^{2+}-free conditions

From these results it seems likely that the rapid, Na^+/Ca^{2+} exchange dependent depletion of the ER stores is responsible for the light-induced rise in cytosolic Ca^{2+} previously reported in ommatidia perfused with Ca^{2+}-free solutions (Peretz et al., 1994; Hardie, 1996; Cook and Minke, 1999; Kohn et al., 2015; Asteriti et al., 2017). It was therefore of interest to explore store depletion in ommatidia under similar Ca_o^{2+}-free conditions. After short-term local perfusion (20–30 s) with Ca^{2+}-free (1 mM EGTA) bath solution, a rapid light-induced store depletion signal was still observed reaching similar low values to those in normal (Ca^{2+} containing) bath, but now with a ~twofold slower time course (Fig. 4*A*,*B*), which would be consistent with the slower kinetics of the light-induced current (and hence Na^+ influx) in Ca^{2+}-free solutions. The time course appeared similar to that of the cytosolic Ca^{2+} rise previously reported in Ca^{2+}-free solutions using GCaMP6f (Asteriti et al., 2017). However, to compare store depletion and cytosolic Ca^{2+} rise directly, we co-expressed the red fluorescent Ca^{2+} indicator, RGECO1 (Dana et al., 2016) together with ER-150 in the same flies and measured store depletion and cytosolic Ca^{2+} rises under Ca^{2+}-free conditions in the same ommatidia. After scaling, the time course of store depletion and cytosolic Ca^{2+} rise overlapped closely, in both cases having a latency of ~200 ms (Fig. 4*C*). Store depletion was largely complete after ~2–3 s, whereas, as would be expected in the absence of further release, after peaking after ~2 s, cytosolic Ca^{2+} monitored by RGECO1 then declined to near baseline levels over the following seconds (Fig. 4*C*). Furthermore we found a strong correlation between the extent of store depletion and the amplitude of the rise in cytosolic Ca^{2+} in the same ommatidia, while the speed of depletion (time to 50% depletion) and cytosolic Ca^{2+} rise were also strongly correlated (Fig. 4*D*,*E*).

Over a longer time course (30 s), ommatidia perfused with Ca^{2+}-free solutions showed the first rapid phase of store refilling, but then levels declined monotonically to levels below those observed in control bath (Fig. 4*F*) . To test the sensitivity of ER store Ca^{2+} to external Ca^{2+} over yet longer periods, ommatidia were perfused with Ca^{2+}-free solution and fluorescence monitored continuously for several minutes. In wild-type flies, ER-150 fluorescence decayed to low levels (~10% of initial value) within ~3 min ($t½$ = 56 s ± 11.4 s, $n = 4$), indicating depletion of the stores to ~20–50 μM, and then recovered quickly ($t½$ =11.4 s ±1.5 s, $n = 4$) on return to normal Ca^{2+} containing bath (Fig. 4*H*). In wild-type flies, such continuous excitation light simultaneously activates the (highly Ca^{2+} permeable) light-sensitive TRP channels; to prevent this, similar measurements were also made in null PLC mutants ($norpA^{P24}$). Store Ca^{2+} still decayed in Ca^{2+}-free bath, but now considerably more slowly ($t½$ = 205 s ± 32 s, $n = 4$). Recovery on return to Ca^{2+} containing bath was still rapid, although slightly slower ($t½$ = 17.5 s ± 1.3 s, n =4) and only partial on the time course of the experiments (Fig. 4*I*).

The dependence of rapid store depletion on CalX or external Na^+ would be most simply explained by Na^+/Ca^{2+} exchange across the ER membrane in response to Na^+ influx via the light-sensitive channels. However, NCX exchangers like CalX are generally assumed to operate only at the plasma membrane. An alternative suggestion might be that the dependence on Na^+/Ca^{2+}exchange was because of some inhibitory effect(s) of the increase in cytosolic $[Ca^{2+}]$, which ensues as a result of failure of the Na^+/Ca^{2+} exchanger to extrude Ca^{2+} across the plasma membrane. If this were the case, one would predict that store depletion would no longer be blocked in ommatidia perfused with solutions lacking Ca^{2+} as well as Na^+. However, once again, rapid store depletion was essentially blocked with perfusion by such 0Ca/0Na solutions, and even the slower phase of decay was less pronounced than in the presence of external Ca^{2+} (Fig. 4*G*). This leaves direct Na^+/Ca^{2+}exchange across the ER membrane as the only obvious explanation for the rapid store depletion, and, given their similar time course, we propose that this accounts for the rise in cytosolic Ca^{2+} observed in Ca^{2+}-free solutions.

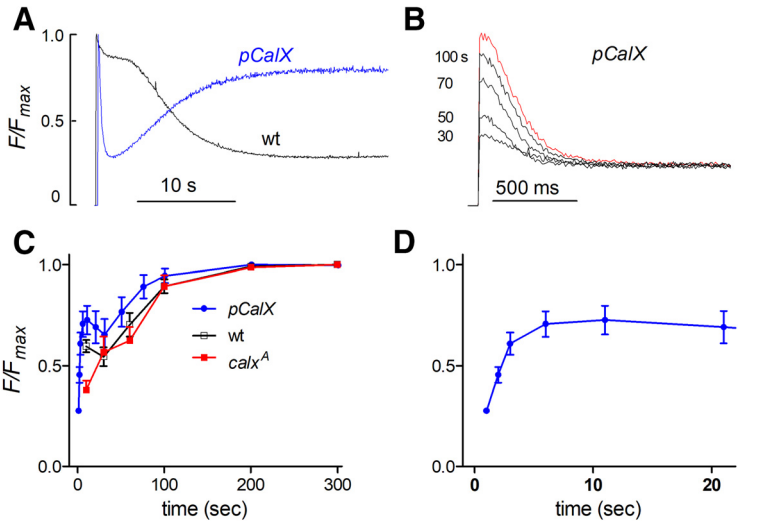

Figure 7. CalX overexpression accelerates and enhances rapid store depletion (*in vivo* DPP). ***A***, ER-150 fluorescence measured *in vivo* from the DPP in intact flies in wild-type and in flies overexpressing the Na^+/Ca^{2+} exchanger (*pCalX*). Rapid depletion was massively enhanced in *pCalx* flies. Following the initial rapid depletion, ER stores in *pCalx* flies showed rapid refilling over 10–20 s during the maintained blue excitation. ***B***, Traces in *pCalX* on faster time scale (*y*-axis scale same as ***A***): red, initially dark adapted and then after 30–100 s in the dark. ***C***, ***D***, time course of store refilling in *pCalX* compared with wild-type: after an initial rapid phase (***D***; *pCalx* data replotted on faster time course), the slower phase of ER store refilling had a similar time course in wild-type, $calx^A$ and *pCalx* flies. However, the fast phase was enhanced in *pCalX*.

Immunolocalization of CalX

Previously CalX has been reported to immuno-localize to the microvillar membrane of the rhabdomeres (Wang et al., 2005b; Halty-deLeon et al., 2018). However, if the rapid store depletion is mediated by Na^+/Ca^{2+} exchange across the ER membrane, then obviously we predict that the CalX exchanger should also be present here. We therefore re-examined CalX immunolocalization using a mutant allele ($calx^B$), which expresses very low levels of CalX (Wang et al., 2005b; Chen et al., 2015) as a negative control for background signal. As previously reported, anti-CalX immunostaining in control flies (w^{1118}) was predominantly observed in the microvillar membrane of the rhabdomeres (Wang et al., 2005b) of both newly eclosed (Fig. 5*A*,*B*) and 1-d-old flies (Fig. 5*E*). In addition, there was less-pronounced, but nevertheless distinct staining on intracellular membranes (Fig. 5). We colabeled the photoreceptor cells with a nuclear stain (TO-PRO-3) and found prominent intracellular signal in the perinuclear area, consistent with ER localization (Fig. 5). Both the rhabdomeral and intracellular signals were absent in $calx^B$ mutants confirming specificity of the antibody (Fig. 5*E*).

To test whether the intracellular CalX staining localized to the ER, we exploited ER-150 as an ER marker, using anti-GFP to recognize ER-150. To eliminate screening pigment autofluorescence from w^+ expression in the ER-150 transgene, we created a tool called the *WE*, which is a transgene that supplies Cas9 and guide RNAs to mutate *mini-*w^+ through Cas9-mediated HDR or NHEJ (Fig. 1; see Materials and Methods). After mutating the *mini-*w^+ associated with the ER-150 transgene with *WE*, we performed double labeling using anti-CalX and anti-GFP. The most prominent anti-GFP (ER-150) staining was again in the perinuclear region, which is a major site for the ER (Fig. 5*C*,*D*) and overall, we found that the intracellular CalX staining largely colocalized with ER-150, supporting the proposal that CalX is present throughout the ER (Fig. 5*C*,*D*).

Monitoring ER Ca^{2+} stores *in vivo*

In order to obtain healthy cells, dissociated ommatidia need to be prepared from newly eclosed flies within ~2–3 h of eclosion (Reuss et al., 1997; Katz et al., 2017). To monitor store $[Ca^{2+}]$ *in vivo* from mature adult flies, we measured ER-150 fluorescence from the DPP of completely intact flies using a low-power (20×) air objective (Satoh et al., 2010; Asteriti et al., 2017). Although the rhabdomere patterns themselves appeared dark in the fluorescent DPP, a diffuse halo of fluorescence emanating from the ER-150 probe generates a large and easily measureable signal in response to the blue excitation (Fig. 6*A*).

While showing similarities to responses observed in dissociated ommatidia, there were also notable differences. Although the fluorescence showed an initial rapid decay with a similar time course to that observed in ommatidia (tau 0.81 ± 0.17 s $n = 14$), the fluorescence now decayed by only ~10% (9.1 ± 0.8%, $n = 14$), cf. ~20–80% in dissociated ommatidia (compare Figs. 3, 6). This fast phase was again largely eliminated in $calx^A$ mutants but not in *itpr*-null mosaic eyes, supporting its identification as Na^+/Ca^{2+} exchange-dependent extrusion from the ER stores. The marked difference in the extent of rapid depletion compared with measurements made in dissociated ommatidia appeared largely to reflect the age of the flies, because DPP measurement made from intact, newly eclosed flies (<2 h) showed much more pronounced (20–50%) rapid depletion and an overall time course more similar to measurements from dissociated ommatidia (Fig. 6*A*,*C*).

Despite the smaller extent of rapid store depletion in intact adult flies, over longer time courses (30 s) there was a second, delayed decay phase with an approximately exponential time constant of 5–10 s (7.0 ± 0.9 s, n =14), which resulted in depletion to levels, on average ~50% of initial F_{max} (range ~20% −80%). This second phase appeared broadly similar in time course and extent to the slow phase seen in dissociated ommatidia from $calx^A$ mutants or after removal of external Na^+. A similar slow phase, albeit further delayed, was also still

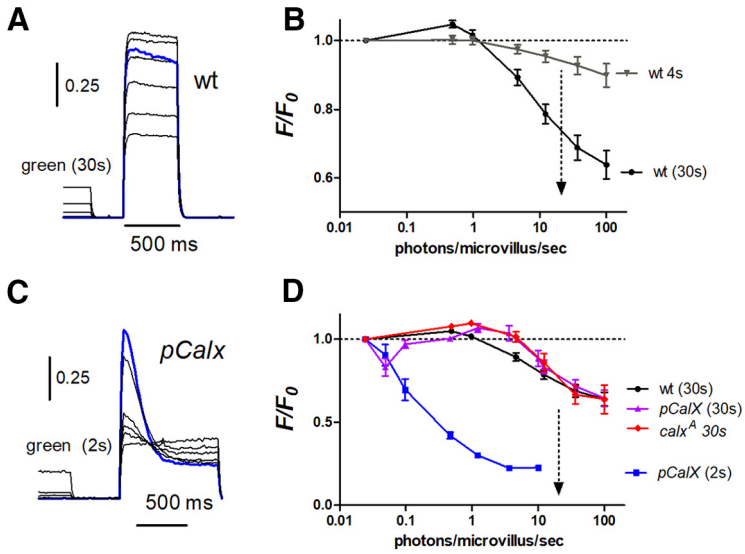

Figure 8. Intensity dependence of store depletion *in vivo* measured from DPP. Flies were pre-illuminated with green light (540 nm) of various intensities for either 2, 4, or 30 s and store Ca^{2+} measured from ER-150 fluorescence immediately afterward. ***A***, ER-150 fluorescence traces from wild-type fly with 30 s green pre-illumination. Blue trace shows initial dark-adapted fluorescence traces (no green pre-illumination). ***B***, intensity dependence of depletion derived from such traces after both 4 s pre-illumination (i.e., monitoring the rapid, CalX-dependent store depletion) and after 30 s (predominantly non-CalX-dependent depletion); intensity expressed in effectively absorbed photons/microvillus/s. Note there was significant store depletion under intensities equivalent to bright daylight (dotted arrow): but at relatively dim intensities there was a slight filling of stores above the dark-adapted levels. ***C***, Traces from fly overexpressing CalX (*pCalX*) with 2 s green pre-illumination. ***D***, intensity dependence of rapid depletion from such traces was sensitized by several orders of magnitude in *pCalx* (*pCalX* 2 s); but after 30 s pre-illumination (which allows for rapid refilling phase; Fig. 7) *pCalX* flies appeared as resistant to depletion as wild-type. $calx^A$ mutants showed behavior broadly similar to wild-type for long (30 s) pre-illumination protocols.

present in DPP measurements from $calx^A$ mutants, and the final level of depletion reached after 30–60 s continuous blue excitation in $calx^A$ was similar or lower than in wild-type (Fig. 6*A*,*D*). The slow phase of depletion was also still detected in *in vivo* measurements of *itpr* mosaic eyes (after mutating the associated mini-w^+ transgene using the white eraser tool). Although on average this appeared to be slightly delayed compared with controls (Fig. 6*A*), this was not significant, indicating that, like the rapid phase, the slow depletion of ER in the photoreceptors does not require $InsP_3$-induced Ca^{2+} release from stores.

After maximal depletion was reached (typically ~50% after 30–60 s), and following M to R photo-reisomerization, fluorescence was re-measured after varying times in the dark. Full recovery of the initial level was obtained after 100–200 s with an exponential time course of ~40–50 s, similar to the slower phase of recovery measured in dissociated ommatidia (Fig. 6*E*,*F*). Although the rapid refilling seen in dissociated ommatidia during maintained blue excitation was not usually observed in dark-adapted flies, a rapid refilling phase was often seen in traces recorded after ~30–60 s of dark adaptation following an episode of blue excitation, as well as in newly eclosed flies (Figs. 6*A*,*E*).

Overexpression of the Na^+/Ca^{2+} exchanger accelerates store depletion

As an additional test for the involvement of Na^+/Ca^{2+} exchange in store depletion, we overexpressed the CalX exchanger using the *ninaE* promoter. Previously we showed that this resulted in a 5- to 8-fold increase in Na^+/Ca^{2+} exchange activity across the plasma membrane (Wang et al., 2005b) and also greatly enhanced the light-induced rise in cytosolic Ca^{2+}, which can be detected in the absence of bath Ca^{2+} (Asteriti et al., 2017). In flies (*pCalX*) overexpressing the CalX exchanger, the depletion of ER stores was also dramatically enhanced and accelerated (Fig. 7*A*). Thus, after a brief delay (~75 ms) ER-150 fluorescence *in vivo* (from the DPP) decayed rapidly to ~25% of the initial level within ~ 1 s, with an exponential time constant of 194 ± 9 ms ($n = 10$), which is ~4× faster than in a wild-type background. In the maintained presence of blue excitation the stores then rapidly refilled (tau ~5 s), probably representing further equilibration of the Na^+/Ca^{2+} exchanger as Na^+ levels subsided following the peak-plateau transition of the response to light and extrusion of Na^+ by Na^+/K^+-ATPase. Further refilling in the dark then proceeded with a similar time course to wild-type (Fig. 7*C*).

Intensity dependence of store depletion

The blue excitation used for monitoring ER-150 fluorescence is a super-saturating stimulus for the photoreceptors. In order to measure store depletion in response to physiologically relevant levels of illumination *in vivo*, we used two-pulse protocols, first stimulating the eye with calibrated green light (λ_{max} 546 nm) of different intensities and then measuring the instantaneous fluorescence. Measurements were made using both 4 s pre-illumination to measure the intensity dependence of the rapid component of depletion, and also with 30 s pre-illumination to include both fast and slow components (Fig. 8). As would be expected from the responses to saturating blue illumination, 4 s pre-illumination resulted in maximally only ~10% depletion, while 30 s pre-illumination induced up to ~40% depletion. The intensity dependences of both components were broadly similar. With relatively modest intensities up to ~30,000 effectively absorbed photons per photoreceptor per second (equivalent to ~1 photon/microvillus/s) there was actually a small (2–5%) but significant increase in fluorescence following long (30 s) pre-illumination, indicative of Ca^{2+} uptake by the stores; however, at higher intensities, the stores became progressively depleted with 50% maximum achievable depletion obtained with ~300,000 photons/s. For reference, full daylight intensities correspond to ~500,000 photons/photoreceptor/s (Juusola et al., 2017), so that substantial depletion can be expected to be occurring in the physiological range. The steady-state reached after 30 s was primarily the result of the slow phase of store depletion mediated by a Na^+/Ca^{2+} exchange independent mechanism, and the intensity dependence of store depletion after 30 s was very similar in $calx^A$ mutants (Fig. 8*D*).

We also measured the intensity dependence of store depletion *in vivo* in *pCalX* flies overexpressing the Na^+/Ca^{2+} exchanger (Fig. 8*C*,*D*). When tested immediately after brief (2 s) pre-adapting flashes, the stores were profoundly depleted in *pCalx* flies by intensities >100× dimmer than those required to deplete stores in wild-type backgrounds. However, when determined using long (30 s) pre-adapting steps of light the stores had clearly refilled during the maintained illumination, and now showed similar intensity dependence to wild-type flies. This suggests that in the short term Na^+/Ca^{2+} exchange results in release of Ca^{2+} from the stores due to the initial surge of Na^+ influx during the peak of the light response, but over the long-term (30 s) as $[Na^+]$

subsides to lower levels following light adaptation, the exchanger actually contributes to refilling the stores.

Lack of substantial store depletion in *trp* mutants

TRP (transient receptor potential) ion channels are so-called because the electrical response to maintained light from photoreceptors in *trp* mutants is transient, decaying to baseline within seconds (Cosens and Manning, 1969; Minke et al., 1975). For many years it was thought that this decay reflected depletion of ER Ca^{2+} stores due the lack of influx via the Ca^{2+}-permeable TRP channels (Minke and Selinger, 1991; Hardie and Minke, 1993; Cook and Minke, 1999). However, an alternative explanation was later proposed when it was found that the decay of the light response was associated with the near total depletion of PIP_2 in the microvillar membrane, explained by the failure of Ca^{2+}-dependent negative feedback to inactivate PLC (Hardie et al., 2001). But whether ER Ca^{2+} stores are depleted in *trp* mutants had never been directly investigated. To address this, we expressed ER-150 in a trp^{343}-null mutant background. Both *in vivo* (DPP) and in dissociated ommatidia, we found that ER Ca^{2+} was actually very resistant to depletion in trp^{343} mutants (Fig. 9). A small (~5–10%) rapid depletion was still observed but with a ~twofold slower time course than that in wild-type controls. There was however no sign of the subsequent slow depletion, and the low levels routinely observed in a wild-type background were never approached. The residual rapid depletion was presumably still mediated by Na^+/Ca^{2+} exchange as it was largely abolished with Na^+ substitution by NMDG in dissociated ommatidia (Fig. 9*A*, *C*). The lack of substantial store depletion in *trp* mutants might suggest that CalX expression on the ER membrane was reduced in *trp* mutants; however, anti-CalX immunostaining of the photoreceptor ER was similar in wild-type controls and trp^{343} mutants (Fig. 9*E*,*F*). A more likely explanation is simply the much reduced net inward current (and hence Na^+ influx) in response to light in *trp* mutants.

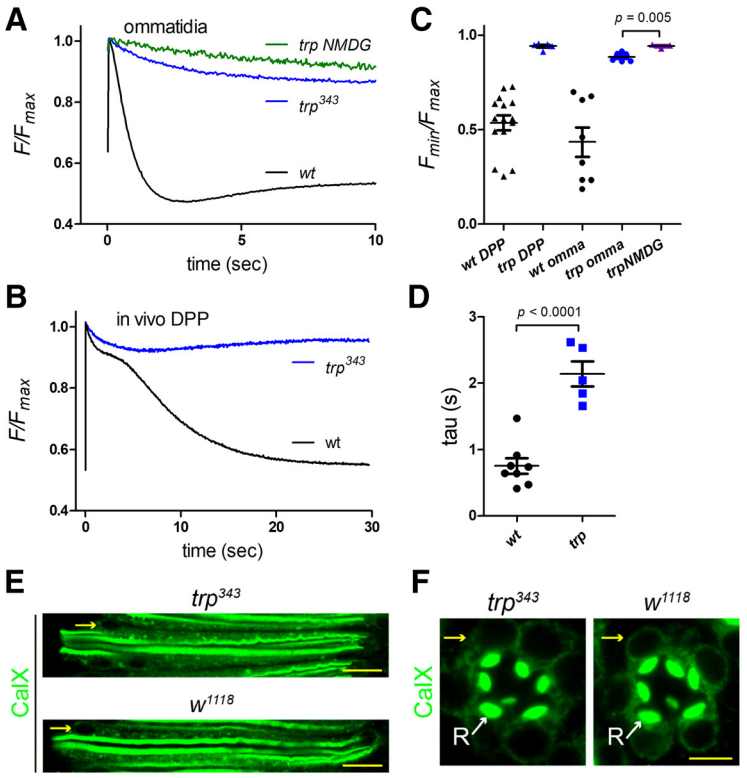

Figure 9. *trp* mutants are resistant to store depletion. ***A***, ER-150 fluorescence in dissociated ommatidia from wild-type (data from Fig. 3) and null trp^{343} mutants (average trace, $n = 6$ ommatidia, 3 flies). Only ~ 10% rapid depletion was detected in *trp*. This was likely still due primarily to Na^+/Ca^{2+} exchange because it was largely prevented by perfusion with $NMDG^+$ substituted for Na^+ (*trp* NMDG). ***B***, Similarly, store depletion measured *in vivo* (from DPP) in *trp* mutants ($n = 6$) was much less pronounced than in wild-type flies. Wild-type data replotted from Figure 6. ***C***, Minimum ER-150 fluorescence values reached in trp^{343} mutants were much less ($p < 0.0001$ on two-tailed *t* tests) than in wild-type (wt); but NMDG perfusion still suppressed depletion further. *In vivo* DPP values are minimum values reached over 30 s; values from dissociated ommatidia (omma) are from rapid depletion phase only (4–10 s). ***D***, Time constant of rapid depletion phase from dissociated ommatidia (single exponential fits) was ~twofold slower in trp^{343} mutants. ***E***, Longitudinal optical sections of ommatidia stained for anti-Calx in trp^{343} and wild-type control (w^{1118}). Scale bar, 10 μm. ***F***, transverse optical sections; yellow arrows, perinuclear ER; white arrows (*R*), rhabdomere. Scale bar, 5 μm.

Discussion

Drosophila phototransduction has long been an influential model for phosphoinositide and Ca^{2+} signaling, but despite much speculation virtually no information is available on the function and roles of ER Ca^{2+} stores. In the present study we measured ER Ca^{2+} levels using a low affinity GCaMP6 variant targeted to the photoreceptor ER lumen, where it generated bright fluorescence throughout the ER network. The probe (ER-GCaMP6-150), originally developed and expressed in mammalian neurons (de Juan-Sanz et al., 2017), has a 45-fold dynamic range, which we confirmed *in situ*, and allows measurements of ER luminal [Ca^{2+}] with excellent signal-to-noise ratio. Not only could we monitor ER Ca^{2+} levels in dissociated ommatidia, it was also straightforward to make *in vivo* measurements from the eyes of completely intact flies. Our results demonstrate rapid light-induced, PLC-dependent depletion of the ER Ca^{2+} stores, which refilled in the dark over a time course of 100–200 s.

Strikingly our results indicate that the rapid light-induced store depletion was mediated by Na^+/Ca^{2+} exchange. *Drosophila* CalX belongs to the NCX family of Na^+/Ca^{2+} exchangers (Schwarz and Benzer, 1997), which are generally considered to act only at the plasma membrane (Blaustein and Lederer, 1999). Although *Drosophila* CalX clearly does function at the plasma membrane (Wang et al., 2005b), our results now provide compelling evidence that it also operates across the ER membrane. To our knowledge NCX activity has not previously been reported on the ER; however, Na^+/Ca^{2+} exchange on internal membranes is not without precedent: for example NCX has been reported on the inner nuclear membrane providing a route for Ca^{2+} transfer between nucleoplasm and the nuclear envelope and hence ultimately the ER network with which it is continuous (Wu et al., 2009). In addition a dedicated mitochondrial Na^+/Ca^{2+} exchanger (NCLX) plays important roles in uptake and release of mitochondrial Ca^{2+} (Palty and Sekler, 2012).

The time course of the Na^+/Ca^{2+}-dependent rapid store depletion in Ca^{2+}-free solutions appeared very similar to the rise in cytosolic Ca^{2+} reported from dissociated ommatidia in Ca^{2+}-

free bath, the source of which has been a subject of debate for over 20 years (Hardie, 1996; Cook and Minke, 1999). It had recently been claimed that this "Ca^{2+}-free rise" was due to $InsP_3$-mediated release from ER Ca^{2+} stores (Kohn et al., 2015); however, we found that it was unaffected in null mutants of the $InsP_3R$ (Asteriti et al., 2017; Bollepalli et al., 2017). Instead, we found that the Ca^{2+}-free cytosolic rise was dependent on Na^+/Ca^{2+} exchange (Asteriti et al., 2017), but it was difficult to understand how this could be mediated by a plasma membrane exchanger when extracellular Ca^{2+} was buffered with EGTA to low nanomolar levels. Our demonstration of rapid Na^+/Ca^{2+}-dependent release of Ca^{2+} from ER with a very similar time course (Fig. 4*C*) now provides an obvious mechanism for this Ca^{2+}-free rise and seems finally to have resolved this long-standing enigma. Interestingly the Na^+/Ca^{2+}-dependent rapid store depletion signal was most pronounced in very young flies around the time of eclosion, as always used in dissociated ommatidia preparations used for Ca^{2+} imaging. Also of note, we found that *trp* mutants were very resistant to depletion, both *in vivo* and in dissociated ommatidia. This argues strongly and directly against the hypothesis that the *trp* decay phenotype reflects depletion of the ER Ca^{2+} stores (Minke and Selinger, 1991; Cook and Minke, 1999).

Although up to ~80% rapid store depletion could be observed in newly eclosed adults, even in 1-d-old flies the rapid store depletion signal *in vivo* was much reduced (to ~10%). However, a much slower depletion was observed in mature adults *in vivo*, and in dissociated ommatidia after Na^+/Ca^{2+} exchange was blocked. The origin of this slow phase depletion remains uncertain: in dissociated ommatidia from young flies this slower depletion was ~50% attenuated, but not blocked in null $InsP_3R$ mutants (*itpr*), whereas *in vivo* measurements of the slow depletion phase in adult *itpr* mutants appeared similar to wild-type. This suggests that although Ca^{2+} release via $InsP_3$ receptors may contribute to the slow depletion in young flies, some other mechanism(s), such as Ca^{2+} release via ryanodine receptors, is largely responsible.

Physiologic roles

Our evidence strongly suggests a novel role for NCX exchangers in mediating Na^+/Ca^{2+} exchange across the ER membrane, but its physiological significance is unclear. Although rapid store depletion was routinely observed under our experimental conditions, the Ca^{2+} released into the cytosol from the ER seems unlikely to play a direct role in phototransduction. First, it has a latency of ~100 ms (cf. ~10 ms for the light-induced current), and second it will in any case be swamped by the much more rapid Ca^{2+} influx via the light-sensitive channels. Thus measurements of cytosolic Ca^{2+} in 0 Ca^{2+} bath indicated a rise to only ~200–300 nM, which compares with much faster rises in the high micromolar range due to direct Ca^{2+} influx via the light-sensitive TRP channels (Hardie, 1996; Oberwinkler and Stavenga, 2000; Asteriti et al., 2017). One possible role for an ER Na^+/Ca^{2+} exchanger would be that it normally operates as a Ca^{2+} uptake mechanism; only briefly giving Ca^{2+} extrusion (and store depletion) following the extreme, and unnatural conditions of many of our experiments; namely, the sudden onset of bright illumination from a dark-adapted state, which results in a massive transient surge of Na^+ influx. Rapid Ca^{2+} uptake (store refilling), presumably via re-equilibration of the exchanger as the initial Na^+ level subsided during the peak-to-plateau transition, was in fact routinely observed during maintained blue illumination (Figs. 3, 6, 7). Furthermore, it is perhaps significant, that despite lacking the rapid depletion phase, the final level of store Ca^{2+} (i.e., after 30 s illumination) in $calx^A$ mutants was if anything lower than that in wild-type backgrounds, although the cytosolic Ca^{2+} levels experienced in $calx^A$ mutants are much higher because of the failure to extrude Ca^{2+} across the plasma membrane (Wang et al., 2005b).

Although store depletion seems unlikely to contribute to activation of the phototransduction cascade, we cannot exclude the possibility that it may play some role in long-term light adaptation. Maintenance of ER Ca^{2+} levels is also important for many other cellular functions including protein folding and maturation in which Ca^{2+} is a cofactor for optimal chaperone activity (Carreras-Sureda et al., 2018). With conspicuously high cytosolic Ca^{2+} levels in the presence of light, photoreceptors face unusual homeostatic challenges and Na^+/Ca^{2+} exchange across the ER may provide an important additional mechanism. In principle the balance between forward and reverse Na^+/Ca^{2+} exchange (i.e., uptake vs release) by an ER Na^+/Ca^{2+} exchanger will depend on the Na^+ gradient across the ER membrane and whether this is actively regulated. To our knowledge there is no information on ER Na^+ levels; although luminal Na^+ in the nuclear envelope (which is continuous with the ER) has been reported to be concentrated (84 mM) in nuclei from hepatocytes by Na/K-ATPase expressed on nuclear membranes (Garner, 2002). Finally, we cannot exclude the possibility that Na^+/Ca^{2+} exchange across the ER might play only a minor physiological role, but is an unavoidable consequence of the presence of functional CalX protein in ER membranes during protein synthesis and targeting. At least this may account for the enhanced depletion signal measured around the time of eclosion when there may be a rapid final phase of protein synthesis for the developing rhabdomere (Hardie et al., 1993).

Conclusion

Our results provide unique insight into ER Ca^{2+} stores in *Drosophila* photoreceptors. The ER-GCaMP6-150 probe lights up an extensive ER network and indicates a high luminal Ca^{2+} concentration probably in excess of 0.5 mM. Our results reveal a rapid, and uniform light-induced depletion of the ER stores mediated by the CalX Na^+/Ca^{2+} exchanger expressed on the ER membrane. The resulting extrusion of Ca^{2+} into the cytosol can readily account for the rise in cytosolic Ca^{2+} observed in dissociated ommatidia in Ca^{2+}-free solutions (Hardie, 1996; Cook and Minke, 1999; Kohn et al., 2015; Asteriti et al., 2017), thus resolving this decades old mystery. In addition to the rapid depletion, we also resolved a much slower depletion that appears to be independent of Na^+/Ca^{2+} exchange and also largely independent of $InsP_3$-induced Ca^{2+} release. The physiological significance of the ER Na^+/Ca^{2+} exchange activity remains uncertain. It is perhaps more likely that it serves as a low affinity Ca^{2+} uptake mechanism supplementing the SERCA pump, and that rapid depletion is only seen during unnatural abrupt bright stimulation from dark-adapted backgrounds leading to massive Na^+ influx and reverse exchange. Ultimately, to resolve the physiological significance of Na^+/Ca^{2+} exchange across the ER membrane it will probably be necessary to selectively disrupt Na^+/Ca^{2+} exchange on the ER without affecting the exchanger on the plasma membrane, which is known to play very important roles in Ca^{2+} homeostasis in the photoreceptors with direct consequences for channel activation and adaptation (Wang et al., 2005b).

References

Acharya JK, Jalink K, Hardy RW, Hartenstein V, Zuker CS (1997) $InsP_3$ receptor is essential for growth and differentiation but not for vision in *Drosophila*. Neuron 18:881–887.

Asteriti S, Liu CH, Hardie RC (2017) Calcium signalling in *Drosophila* photoreceptors measured with GCaMP6f. Cell Calcium 65:40–51.

Blaustein MP, Lederer WJ (1999) Sodium calcium exchange: its physiological implications. Physiol Rev 79:763–854.

Bollepalli MK, Kuipers ME, Liu CH, Asteriti S, Hardie RC (2017) Phototransduction in *Drosophila* is compromised by Gal4 expression but not by $InsP_3$ Receptor knockdown or mutation. eNeuro 4:ENEURO.0143-17.2017.

Carreras-Sureda A, Pihán P, Hetz C (2018) Calcium signaling at the endoplasmic reticulum: fine-tuning stress responses. Cell Calcium 70:24–31.

Chen Z, Chen HC, Montell C (2015) TRP and rhodopsin transport depends on dual XPORT ER chaperones encoded by an operon. Cell Rep 13:573–584.

Cook B, Minke B (1999) TRP and calcium stores in *Drosophila* phototransduction. Cell Calcium 25:161–171.

Cosens DJ, Manning A (1969) Abnormal electroretinogram from a *Drosophila* mutant. Nature 224:285–287.

Dana H, Mohar B, Sun Y, Narayan S, Gordus A, Hasseman JP, Tsegaye G, Holt GT, Hu A, Walpita D, Patel R, Macklin JJ, Bargmann CI, Ahrens MB, Schreiter ER, Jayaraman V, Looger LL, Svoboda K, Kim DS (2016) Sensitive red protein calcium indicators for imaging neural activity. eLife 5:e12727.

de Juan-Sanz J, Holt GT, Schreiter ER, de Juan F, Kim DS, Ryan TA (2017) Axonal endoplasmic reticulum Ca^{2+} content controls release probability in CNS nerve terminals. Neuron 93:867–881.e6.

Fain GL, Hardie R, Laughlin SB (2010) Phototransduction and the evolution of photoreceptors. Curr Biol 20:R114–R124.

Garner MH (2002) Na,K-ATPase in the nuclear envelope regulates Na^+: k^+ gradients in hepatocyte nuclei. J Membr Biol 187:97–115.

Halty-deLeon L, Hansson BS, Wicher D (2018) The *Drosophila* melanogaster Na^+/Ca^{2+} Exchanger CALX controls the Ca^{2+} level in olfactory sensory neurons at rest and after odorant receptor activation. Front Cell Neurosci 12:186.

Hardie RC (1996) INDO-1 measurements of absolute resting and light-induced Ca^{2+} concentration in *Drosophila* photoreceptors. J Neurosci 16:2924–2933.

Hardie RC (2011) A brief history of trp: commentary and personal perspective. Pflugers Arch 461:493–498.

Hardie RC (2012) Phototransduction mechanisms in *Drosophila* microvillar photoreceptors. WIRES Membr Transp Signal 1:162–187.

Hardie RC, Juusola M (2015) Phototransduction in *Drosophila*. Curr Opin Neurobiol 34:37–45.

Hardie RC, Minke B (1992) The trp gene is essential for a light-activated Ca^{2+} channel in *Drosophila* photoreceptors. Neuron 8:643–651.

Hardie RC, Minke B (1993) Novel Ca^{2+} channels underlying transduction in *Drosophila* photoreceptors: implications for phosphoinositide-mediated Ca^{2+} mobilization. Trends Neurosci 16:371–376.

Hardie RC, Peretz A, Pollock JA, Minke B (1993) Ca^{2+} limits the development of the light response in *Drosophila* photoreceptors. Proc Biol Sci 252:223–229.

Hardie RC, Raghu P, Moore S, Juusola M, Baines RA, Sweeney ST (2001) Calcium influx via TRP channels is required to maintain PIP_2 levels in *Drosophila* photoreceptors. Neuron 30:149–159.

Hardie RC, Liu CH, Randall AS, Sengupta S (2015) *In vivo* tracking of phosphoinositides in *Drosophila* photoreceptors. J Cell Sci 128:4328–4340.

Juusola M, Dau A, Song Z, Solanki N, Rien D, Jaciuch D, Dongre SA, Blanchard F, de Polavieja GG, Hardie RC, Takalo J (2017) Microsaccadic sampling of moving image information provides *Drosophila* hyperacute vision. eLife 6:e26117.

Katz B, Minke B (2009) *Drosophila* photoreceptors and signaling mechanisms. Front Cell Neurosci 3:2.

Katz B, Gutorov R, Rhodes-Mordov E, Hardie RC, Minke B (2017) Electrophysiological method for whole-cell voltage clamp recordings from *Drosophila* photoreceptors. J Vis Exp 124:e55627.

Katz B, Minke B (2018) The *Drosophila* light-activated TRP and TRPL channels: targets of the phosphoinositide signaling cascade. Prog Retin Eye Res 66:200–219.

Kohn E, Katz B, Yasin B, Peters M, Rhodes E, Zaguri R, Weiss S, Minke B (2015) Functional cooperation between the IP3 receptor and phospholipase C secures the high sensitivity to light of *Drosophila* photoreceptors *in vivo*. J Neurosci 35:2530–2546.

Minke B, Wu C, Pak WL (1975) Induction of photoreceptor voltage noise in the dark in *Drosophila* mutant. Nature 258:84–87.

Minke B, Selinger Z (1991) Inositol lipid pathway in fly photoreceptors: excitation, calcium mobilization and retinal degeneration. Prog Retinal Res 11:99–124.

Minke B (2010) The history of the *Drosophila* TRP channel: the birth of a new channel superfamily. J Neurogenet 24:216–233.

Montell C, Rubin GM (1989) Molecular characterization of *Drosophila* trp locus, a putative integral membrane protein required for phototransduction. Neuron 2:1313–1323.

Montell C (2011) The history of TRP channels, a commentary and reflection. Pflugers Arch 461:495–506.

Montell C (2012) *Drosophila* visual transduction. Trends Neurosci 35:356–363.

Niemeyer BA, Suzuki E, Scott K, Jalink K, Zuker CS (1996) The *Drosophila* light-activated conductance is composed of the two channels TRP and TRPL. Cell 85:651–659.

Oberwinkler J, Stavenga DG (2000) Calcium transients in the rhabdomeres of dark- and light-adapted fly photoreceptor cells. J Neurosci 20:1701–1709.

Palty R, Sekler I (2012) The mitochondrial Na^+/Ca^{2+} exchanger. Cell Calcium 52:9–15.

Pearn MT, Randall LL, Shortridge RD, Burg MG, Pak WL (1996) Molecular, biochemical, and electrophysiological characterization of *Drosophila* norpA mutants. J Biol Chem 271:4937–4945.

Peretz A, Suss-Toby E, Rom-Glas A, Arnon A, Payne R, Minke B (1994) The light response of *Drosophila* photoreceptors is accompanied by an increase in cellular calcium: effects of specific mutations. Neuron 12:1257–1267.

Raghu P, Colley NJ, Webel R, James T, Hasan G, Danin M, Selinger Z, Hardie RC (2000) Normal phototransduction in *Drosophila* photoreceptors lacking an $InsP_3$ receptor gene. Mol Cell Neurosci 15:429–445.

Randall AS, Liu CH, Chu B, Zhang Q, Dongre SA, Juusola M, Franze K, Wakelam MJ, Hardie RC (2015) Speed and sensitivity of phototransduction in *Drosophila* depend on degree of saturation of membrane phospholipids. J Neurosci 35:2731–2746.

Reuss H, Mojet MH, Chyb S, Hardie RC (1997) *In vivo* analysis of the *Drosophila* light-sensitive channels, TRP and TRPL. Neuron 19:1249–1259.

Rosenbaum EE, Hardie RC, Colley NJ (2006) Calnexin is essential for rhodopsin maturation, Ca^{2+} regulation, and photoreceptor cell survival. Neuron 49:229–241.

Satoh AK, Xia H, Yan L, Liu CH, Hardie RC, Ready DF (2010) Arrestin translocation is stoichiometric to rhodopsin isomerization and accelerated by phototransduction in *Drosophila* photoreceptors. Neuron 67:997–1008.

Schrag JD, Bergeron JJ, Li Y, Borisova S, Hahn M, Thomas DY, Cygler M (2001) The Structure of calnexin, an ER chaperone involved in quality control of protein folding. Mol Cell 8:633–644.

Schwarz EM, Benzer S (1997) Calx, a Na-Ca exchanger gene of *Drosophila* melanogaster. Proc Natl Acad Sci U S A 94:10249–10254.

Scott K, Sun YM, Beckingham K, Zuker CS (1997) Calmodulin regulation of *Drosophila* light-activated channels and receptor function mediates termination of the light response *in vivo*. Cell 91:375–383.

Sengupta S, Barber TR, Xia H, Ready DF, Hardie RC (2013) Depletion of $PtdIns(4,5)P_2$ underlies retinal degeneration in *Drosophila* trp mutants. J Cell Sci 126:1247–1259.

Stark WS, Sapp R, Carlson SD (1989) Photoreceptor maintenance and degeneration in the Norpa (no receptor potential-a) mutant of *Drosophila melanogaster*. J Neurogenet 5:49–59.

Stowers RS, Schwarz TL (1999) A genetic method for generating *Drosophila* eyes composed exclusively of mitotic clones of a single genotype. Genetics 152:1631–1639.

Venkatesh K, Hasan G (1997) Disruption of the IP3 receptor gene of *Drosophila* affects larval metamorphosis and ecdysone release. Curr Biol 7:500–509.

Voolstra O, Huber A (2020) Ca^{2+} signaling in *Drosophila* photoreceptor cells. Adv Exp Med Biol 1131:857–879.

Wang T, Jiao Y, Montell C (2005a) Dissecting independent channel and scaffolding roles of the *Drosophila* transient receptor potential channel. J Cell Biol 171:685–694.

Wang T, Xu H, Oberwinkler J, Gu Y, Hardie RC, Montell C (2005b) Light activation, adaptation, and cell survival functions of the Na^+/Ca^{2+} exchanger CalX. Neuron 45:367–378.

Wu G, Xie X, Lu ZH, Ledeen RW (2009) Sodium-calcium exchanger complexed with GM1 ganglioside in nuclear membrane transfers calcium from nucleoplasm to endoplasmic reticulum. Proc Natl Acad Sci U S A 106:10829–10834.